Electronic Supplementary Material (ESI) for RSC Sustainability.

Supplementary Information

Guanidine Functionalized Porous SiO_2 as Heterogeneous Catalysts for Microwave Depolymerization of PET and PLA

Éadaoin Casey[1,2], Rachel Breen[1,2], Gerard Pareras Niell[3], Albert Rimola[3], Justin. D Holmes[1,2], Gillian Collins[1,2]*

[1] School of Chemistry, University College Cork, Cork, T12 YN60, Ireland.

[2] AMBER Centre, Environmental Research Institute, University College Cork, Cork, T23 XE10, Ireland.

[3]Departament de Química, Universitat Autònoma de Barcelona, 08193 Bellaterra, Catalonia, Spain.

1. Introduction

Table S1

Catalyst	**PET:Cat**	**Conditions**	**BHET Yield %**	***Reference***
[Ch][OAc]	5 wt%	180 °C, 240 min	85.2	[1]
[bmim]Cl	80 wt%	180 °C, 480 min	41.6	[2]
Urea	10 wt%	180 °C, 180 min	78	[3]
[Bmim]OH	5 wt%	190 °C, 120 min	71.2	[4]
TBD: MSA salt	0.5 eq	180 °C, 120 min	91	[5]
t-BuP_2	2.4 wt%	190 °C, 90 min	92.7	[6]
$[Ch]_3[PO_4]$	90 wt%	120 °C, 180 min	60.6	[7]
[Ch][Gly]	5 wt%	150 °C, 6 h	51	[8]
TBD based protic ionic salts	20 wt%	190 °C, 120 min	83.5	*[9]*
cyanamide	5 wt%	190 °C, 150 min	95.2	*[10]*

2. Experimental

Chemicals

Mesoporous cellular foam (MCF) SiO_2 was obtained from Glantreo. (APTES), N,N dicyclohexylcarbodimine (DCC), 1-ethyl-3-(3-dimethylaminopropyl) carbodiimide (EDC), dicyandiamide (DCD) , methanol, ethanol, toluene, tetrahydrofuran and ethylene glycol were all purchased from Sigma Aldrich. PET was obtained from post-consumer water bottles after lids and labels were removed. Commercial PLA was obtained from Vegware lids. The plastics were cut into 1 mm x 1 mm pieces for glycolysis and methanolysis experiments. Repeating unit of 192.68 g/mol was used as the molecular weight of PET.

2.1 Synthesis of SiO_2-DCG

In a 100 ml round bottom flask, 10 mmol of the guanidine precursor, N,N dicylcohexylcarbodimine (DCC), 1-ethyl-3-(3-dimethylaminopropyl) carbodiimide (EDC) or dicyandiamide (DCD) was dissolved in 20 ml of dry toluene under argon. 2.1 ml of 3-aminopropyltriethoxylsilane (APTES) was added, and the reaction was refluxed at 100 °C for 24 h under Ar. Next 1 g of SiO_2 was added and the reaction was left to refluxed for a further 24 h. When the reaction had completed, the resulting mixture was filtered and washed with copious amounts of ethanol and the product and dried at 60°C in an oven.

2.2 Thermal glycolysis of PET

In a typical procedure, 1 g of PET, 0.1 g catalyst and 5 ml of ethylene glycol were refluxed at 190 °C for 3 h. The mass of catalyst refers to the mass of the SiO2 and the guanidine ligand, which is equivalent 2 wt% with respect to the guanidine. Once reaction was complete, 5 ml of ice-cold H_2O was added to the reaction, filtered off and dried. The catalyst was separated by filtration. The filtrate was placed in the fridge overnight after which the BHET crystallised out the solution. The BHET crystals were

collected be filtration, washed with water and dried overnight before being weighed to calculate the % yield. PET conversion and yield were calculated by the equations below.

% Conversion of PET: $\frac{W_0 - W_1}{W_0} x\ 100$ **eqn. 1**

Where W_0 is the initial weight of the PET used and W_1 is the weight of the unreacted PET after the reaction.

% Yield of BHET: $\frac{W_{BHET}/M_{BHET}}{W_0/M_{PET}} x\ 100$ **eqn. 2**

Where, W_{BHET} is weight of the BHET product after recrystallisation, M_{BHET} is the molecular weight of BHET, W_0 is the initial weight of PET used and M_{PET} is the repeating unit of PET (192.68 g/mol).

2.3 Microwave assisted glycolysis of PET

Initial MW assisted reaction were carried out under the same conditions as the thermally heated reactions, followed by an optimization study as detailed in Table S3. Optimal conditions were found to be 1 g of PET, 0.1 g catalyst and 10 ml ethylene glycol were added to the Milestone Flexiwave SK-15 high pressure digestion rotors and the reactions were carried out at between 10-60 min ranging from 190-220 °C with a stir speed of 960 rpm, ramp time of 5 min and at 800 W. The recrystallization step post-reaction was the same as for thermal glycolysis.

2.4 Methanolysis of PLA

0.5 g PLA, 50 mg catalyst, 5 ml MeOH and 7.5 ml of tetrahydrofuran (THF) was placed in an autoclave and sealed tight, which was then placed into oven at 130 °C for 20 h. Once reaction was complete, the resulting mixture was filtered and washed with excess MeOH, and the solvent was removed via rotary evaporation leaving the product MeLa. The unreacted plastic was collected from the filter paper, dried and weighed to calculate the PLA mass loss.

2.5 Microwave assisted methanolysis of PLA

0.5 g PLA, 50 mg catalyst, and a ratio of 2:3 methanol : THF were added to Teflon tubes and reacted in a Flexiwave microwave at 130 °C with a ramp time of 5 min for times ranging from 10-60 min and at 800 W.

% Conversion of PLA: $\frac{W_0 - W_1}{W_0} x\ 100$ **eqn. 3**

Where W_0 is the initial weight of the PLA used and W_1 is the weight of the unreacted PLA after the reaction.

3. Materials Characterisation

Scanning electron microscopy (SEM) was performed using a FEI Quanta 650 SEM at an accelerating voltage of 5 kV. The samples were gold coated using a Quorum 150T S magnetron sputtering system as they were non-conductive. X-ray Photoelectron Spectroscopy (XPS) was acquired using a KRATOS AXIS 165 monochromatized X-ray photoelectron spectrometer equipped with an Al Kα (hv = 1486.6 eV) X-ray source. Spectra were collected at a take-off angle of 90° and all spectra were referenced to the C 1s peak at 284.8 eV. Transmission electron microscopy (TEM) analysis was performed using a JEOL 2100 electron microscope at an operating voltage of 200 kV. Fourier transform infrared (FTIR) spectra were recorded on a Perkin Elmer Spectrum Two FT-IR Spectrometer operating in the range of 4000-450 cm^{-1} with a resolution of 4 cm^{-1} and spectra were averaged from 20 scans. BET sorption analysis was performed on a Micromeritics Tristar II surface area and porosity analyser. Prior to analysis, each sample was degassed for 3 h at 400 °C and measurements were performed at -169.15 °C (77 K). The surface area was determined using the BET (Brunauer-Emmett-Teller) method. The pore volume, pore diameter and pore size distribution were determined using the BJH (Barrett-Joyner-Halenda) method.[11] Termogravimetric analysis (TGA) was carried out on a TA Instruments Thermogravimetric Analyzer TGA Q500 V20.13 Build 39. Nuclear magnetic resonance (NMR) samples

were run in deuterated chloroform ($CDCl_3$). 1H NMR spectra were recorded on Bruker Avance III 300 NMR spectrometers, in proton-coupled mode using tetramethylsilane (TMS) as the internal standard. Microwave reactions were performed in Teflon vessels in a milestone Flexiwave microwave synthesis platform with a SK-15 high pressure rotor equipped with an IR temperature sensor.

4. Computational details

Density functional theory (DFT) simulations were carried out using the CP2K package.[12] The mesoporous SiO_2 structure used in the experiments was computationally represented as a periodic amorphous silica (SiO_2) surface. The chosen SiO_2 surface presents a silanol density of 7.2 OH/nm^2 assuring the maximum number of Si atoms available to be functionalized in the unit cell.[13] For the initial bare SiO_2 surface, both internal atomic positions and cell parameters were optimized (resulting with dimensions of a=13.34 Å, b=13.73 Å and c=49.21 Å, in which the last one represents an empty space between surface replicas). The rest of the optimizations (namely, with the ligands and to simulate reactivity) were performed only relaxing the atomic positions keeping the cell parameters fixed. Geometry optimizations were carried out using the semi-local Perdew–Burke–Ernzerhof (PBEsol) functional[14], combined with a double-ζ basis set (DZVP-MOLOPT-SR-GTH gaussian basis set) for all the atom types, together with the Grimme's D3(BJ) dispersion correction to the potential energy,[15] and a cutoff set at 500 Ry for the plane wave auxiliary basis set. Core electrons were described with the Goedecker–Teter–Hutter pseudopotentials[16] and valence ones with a mixed Gaussian and plane-wave (GPW) approach.[17] Solvation effects were considered by performing single point energy calculations on the optimized systems adopting the self-consistent continuum solvation (SCCS) model as implemented in CP2K, aiming to reproduce the experimental conditions of ethylene glycol (EG) and tetrahydrofuran (THF) as solvents.[18]

Finally, to determine the nature of the stationary points of the potential energy surfaces (i.e., local minima and saddle points) the corresponding vibrational harmonic frequencies were calculated at the PBE-D3BJ/DZVP level using the finite differences method. For frequency calculations, a partial Hessian

approach was used to reduce the computational cost of the calculations and the vibrational frequencies were calculated on only on a fragment of the system that represents the most chemically relevant part, *i.e.*, the reactive atoms and the surface site.

Table S2: BET analysis of bare SiO_2, SiO_2-DCG, SiO_2-EDG and SiO_2-DCD catalysts.

	Surface Area m^2g^{-1}	**Pore diameter** (Å)	**Pore volume** cm^3g^{-1}
SiO_2	412.4	108	0.5342
SiO_2 -DCG	182.2	100	0.4247
SiO_2-EDG	101.8	90	0.4778
SiO_2-DCD	38.4	84	0.1711

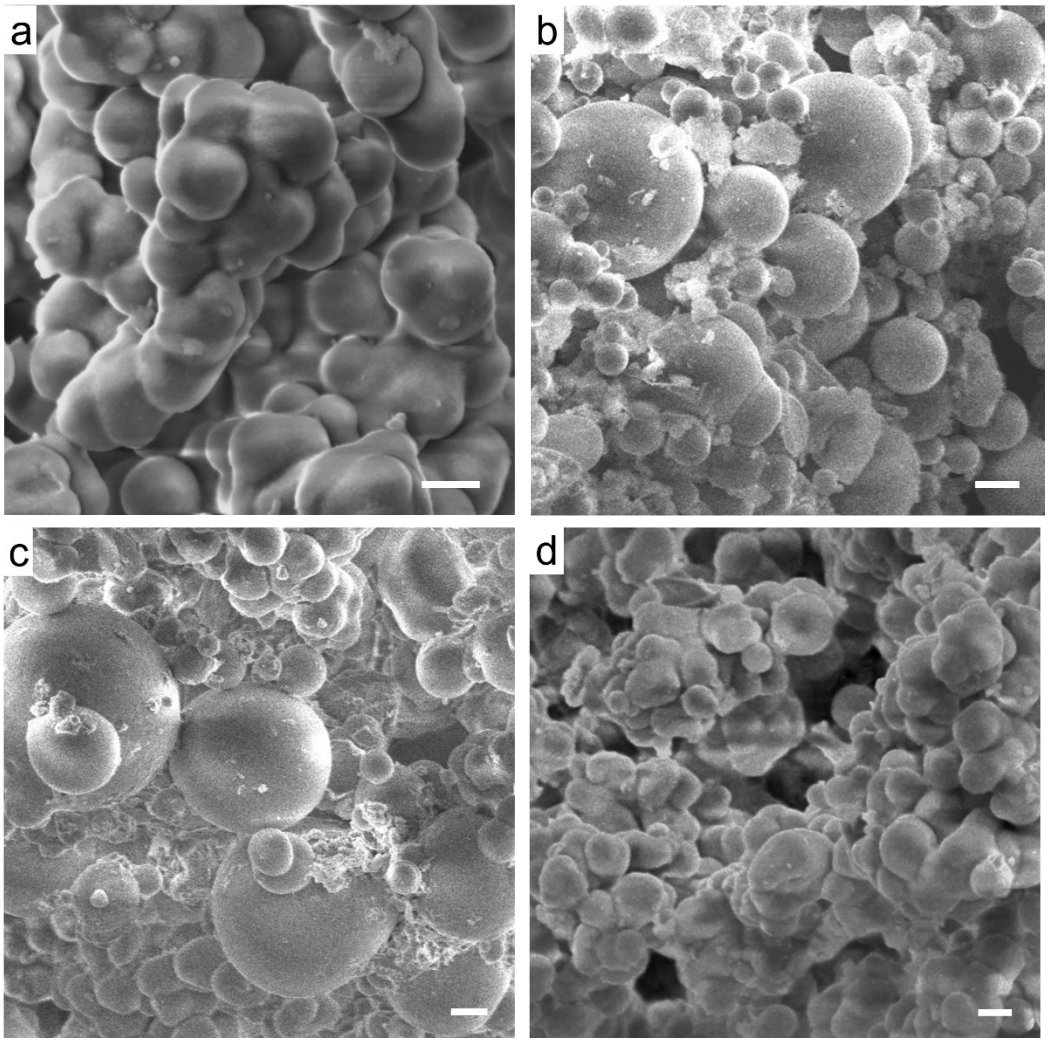

Figure S1: SEM images of (a) bare SiO_2 and after functionalization with the (b) DCG (c) EDG and (d) DCD ligands.

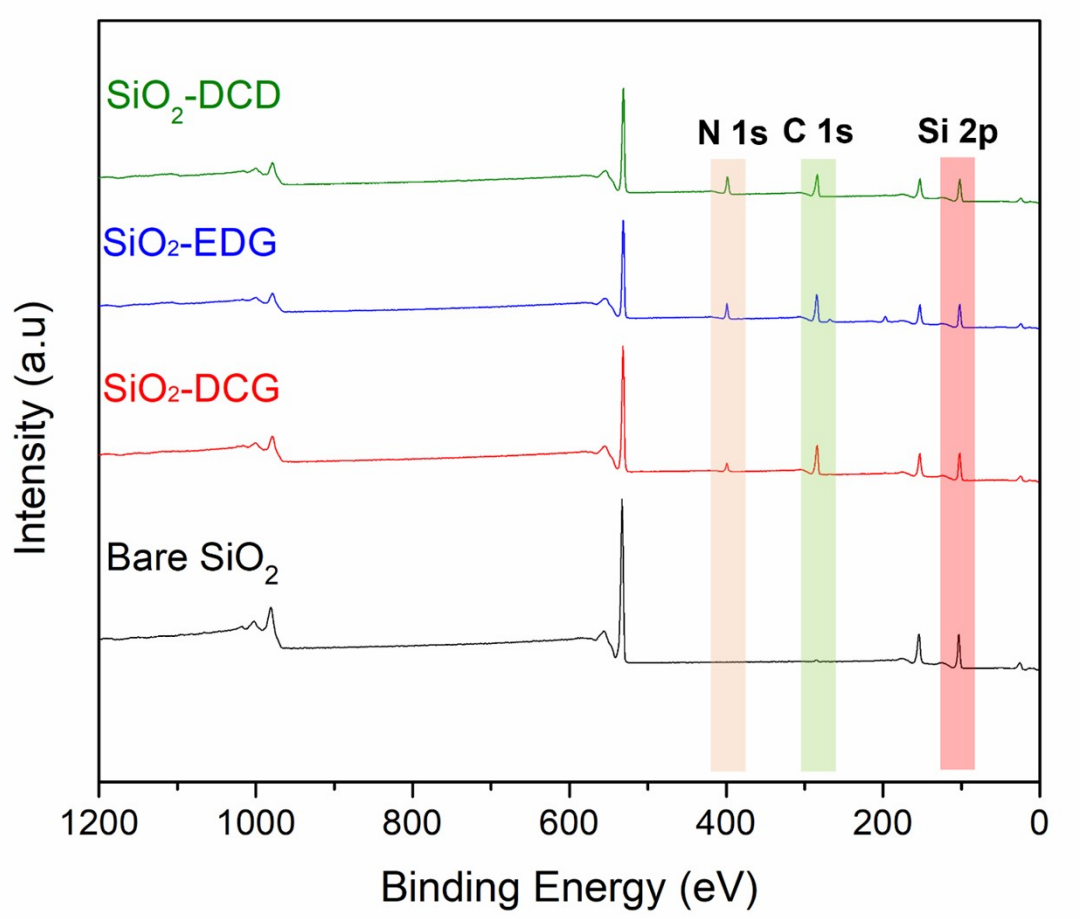

Figure S2: XPS Survey scan for bare SiO_2, SiO_2-DCG, SiO_2-EDG and SiO_2-DCD catalysts.

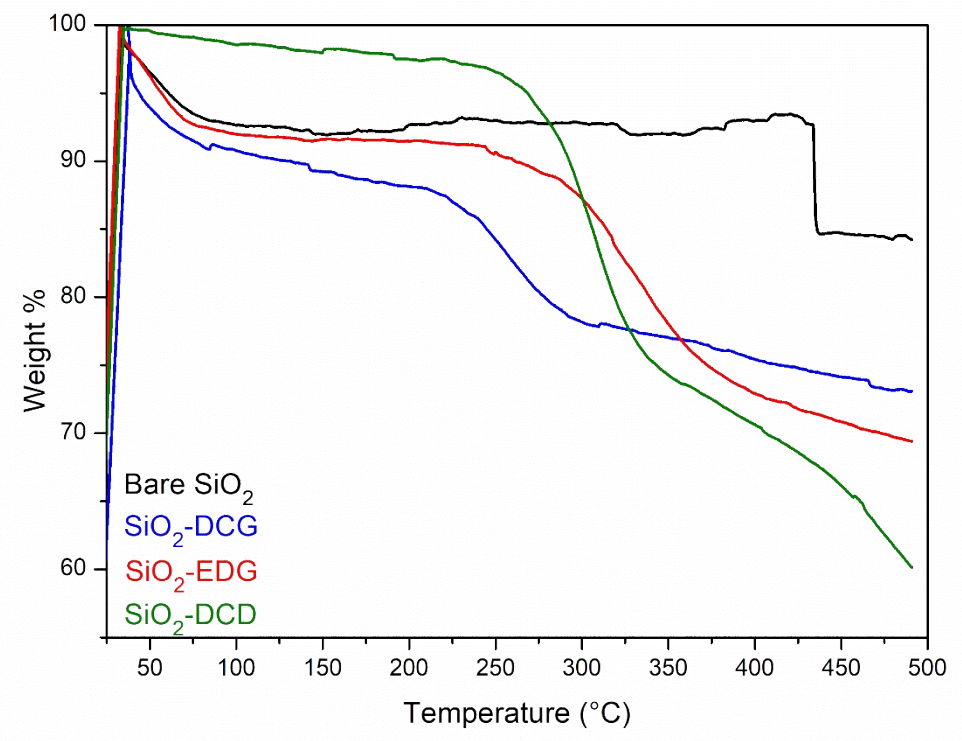

Figure S3: Thermogravimetric analysis of bare SiO_2, SiO_2-DCG, SiO_2-EDG and SiO_2-DCD.

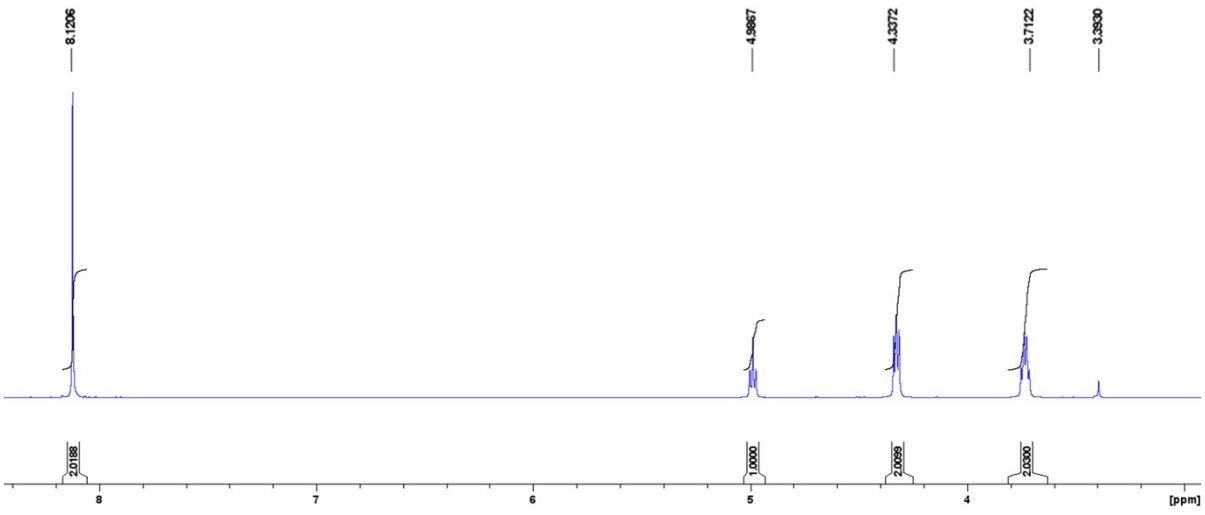

Figure S4: 1H NMR of the product BHET

NMR analysis confirmed that no formation of dimers or oligomers occurred and that BHET was the only product formed in the reaction. The 1H NMR spectrum of BHET can be seen in figure S5, where

the four main peaks were a singlet at 8.12 ppm corresponding to an aromatic ring, an OH triplet at 4.96 ppm, CH_2 triplet at 4.33 ppm and CH_2 quartet at 3.71 ppm. Residual solvent d_6-DMSO was located at 2.51 ppm. The results are in good agreement with literature values of BHET.

Table S3: Optimization of microwave PET depolymerization parameters.

Catalyst	Time	Stir Speed	Temperature	Conversion PET
No catalyst	40 min	960 rpm	190 °C	0 %
No catalyst	40 min	960 rpm	210 °C	10 %
SiO2 (bare)	40 min	960 rpm	190 °C	10 %
SiO2 (bare)	40 min	960 rpm	210 °C	30 %
SiO_2-DCG	30 min	960 rpm	190 °C	6 %
SiO_2-DCG	30 min	960 rpm	200 °C	20 %
SiO_2-DCG	30 min	960 rpm	210 °C	50 %
SiO_2-DCG	40 min	960 rpm	210 °C	81 %
SiO_2-DCD	30 min	960 rpm	190 °C	23 %
SiO_2-DCD	30 min	960 rpm	200 °C	39 %
SiO_2-DCD	30 min	960 rpm	210 °C	93 %
SiO_2-DCD	40 min	960 rpm	210 °C	100 %
SiO_2-DCD	40 min	256 rpm	210 °C	85 %
SiO_2-EDG	30 min	960 rpm	190 °C	4 %
SiO_2-EDG	30 min	960 rpm	200 °C	16 %
SiO_2-EDG	30 min	960 rpm	210 °C	85 %
SiO_2-EDG	40 min	960 rpm	210 °C	100 %

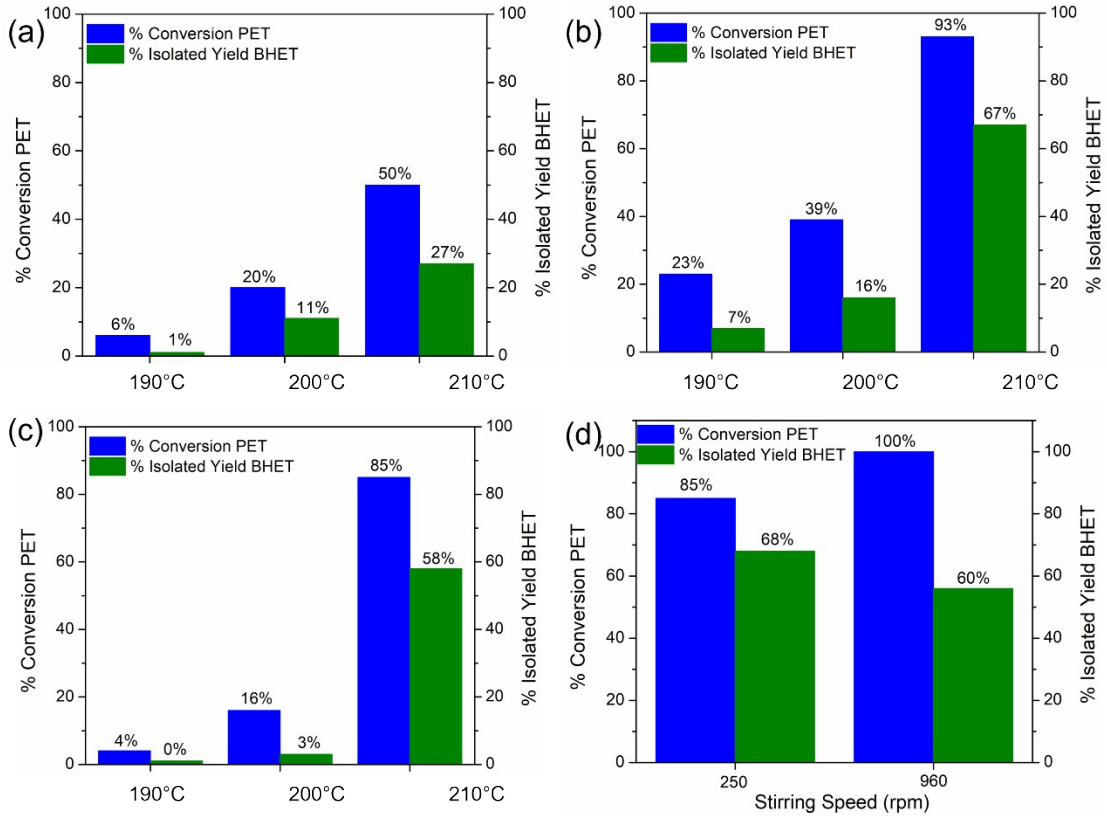

Figure S5: Microwave assisted glycolysis of PET under different reaction temperatures for (a) SiO_2-DCG, (b) SiO_2-EDG and (c) SiO_2-DCD and catalysts (d) Stir speed optimization.

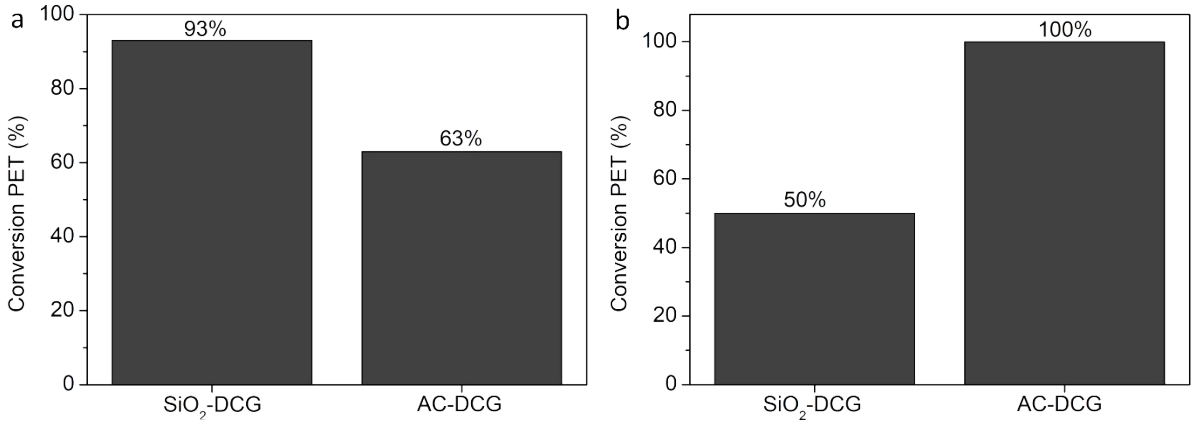

Figure S6: Comparison of PET glycolysis using DCG ligands supported on activated carbon and SiO_2 using a) conventional heating at a temperature of 190 °C and b) microwave-assisted heating at a temperature of 210 °C.

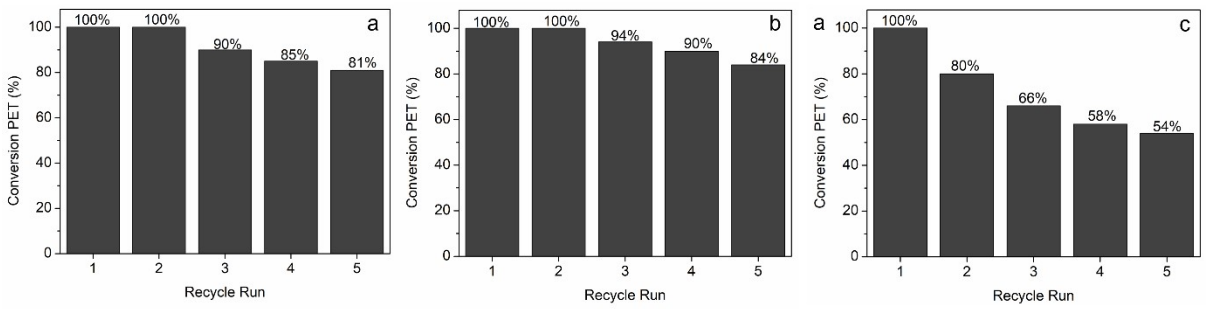

Figure S7: Recyclability performance of the SiO_2-DCD catalyst under optimised thermal conditions and (b) optimised MW conditions (c) SiO_2-DCG catalyst under thermal conditions.

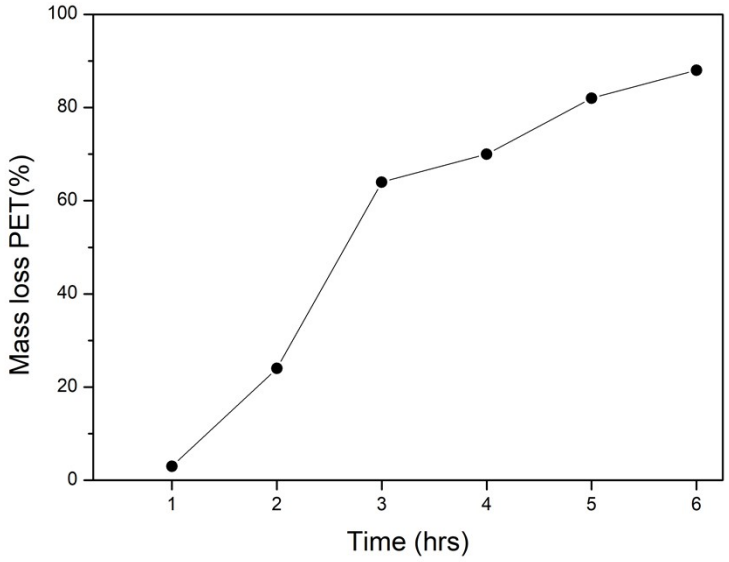

Figure S8: Time series of mass loss PET using 1,4 butanediol as a solvent.

Table S4: Reaction optimization of methanolysis of PLA under microwave irradiation.

Catalyst	MeOH	THF	Temp	Time	Stirring	Mass Loss PLA	Oligomers	MeLa
EDG	2 ml	3 ml	80 °C	30 min	256 rpm	0 %	-	-
DCD	2 ml	3 ml	80 °C	30 min	256 rpm	35 %	-	-
DCG	2 ml	3 ml	80 °C	30 min	960 rpm	14 %	-	-
EDG	2 ml	3 ml	80 °C	30 min	960 rpm	5 %	-	-
DCD	2 ml	3 ml	80 °C	30 min	960 rpm	7 %	-	-
DCG	5 ml	-	130 °C	30 min	960 rpm	96 %	100 %	trace
DCG	2 ml	3 ml	130 °C	30 min	960 rpm	96 %	100 %	trace
DCG	1 ml	4 ml	130 °C	30 min	960 rpm	91 %	100 %	trace

EDG	2 ml	3 ml	130 °C	30 min	960 rpm	84 %	100 %	-
DCG	2 ml	3 ml	130 °C	30 min	960 rpm	100 %	70 %	30%
DCD	2 ml	3 ml	130 °C	30 min	960 rpm	97 %	70 %	12 %
DCG	2 ml	3 ml	130 °C	90 min	960 rpm	100 %	68 %	30%

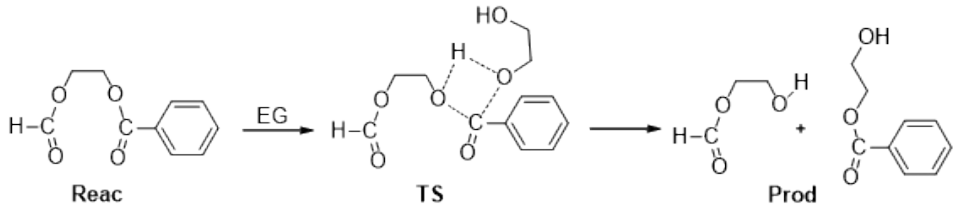

Figure S9. Reaction model used for the benchmarking study.

Table S5. Computed relative energies (in kcal mol^{-1}) for the reaction model used in the benchmarking study. Optimized geometries were carried out at PBE-D3(BJ)/DZVP theory level and single point energy calculations at DLPNO-CCSD(T). In parenthesis, the relative error (in %) for the potential energy barrier is also shown.

System	PBE/DZVP	DLPNO-CCSD(T)
Reac	0.00	0.00
TS	36.05	37.79 (4.6%)
Prod	-7.22	-5.36

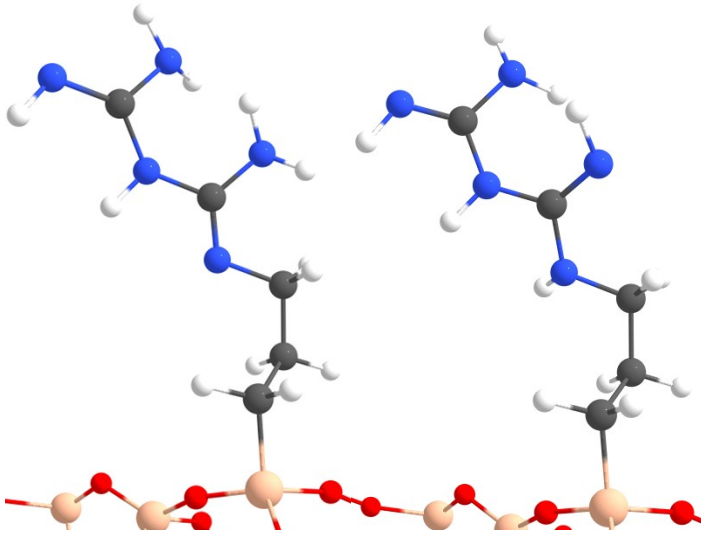

(a) **(b)**

Figure S10 (a): Optimized structure for the SiO_2-DCD tautomer with one primary amine, two secondary amine and two imines. **(b)** Optimized structure for the DCD@SiO_2 tautomer with two primary amines, one secondary amine and two imines. Colour scheme: grey for C, red for O, white for H, blue for N and beige for Si.

Table S6. Collected the relative Gibbs energies at 190 °C in kcal mol^{-1} for the uncatalyzed PET depolymerization reaction considering 1, 2, 3 and 4 units of ethylene glycol (EG) involved in the transition state.

System	**1 EG** *kcal mol^{-1}*	**2 EG** *kcal mol^{-1}*	**3 EG** *kcal mol^{-1}*	**4EG** *kcal mol^{-1}*
1	0.00	0.00	0.00	0.00
TS_{1-2}	24.26	19.29	17.06	16.43
2	12.82	12.82	12.82	12.82

1. Y. Liu, X. Yao, H. Yao, Q. Zhou, J. Xin, X. Lu and S. Zhang, *Green Chemistry*, 2020, **22**, 3122-3131.
2. H. Wang, Y. Liu, Z. Li, X. Zhang, S. Zhang and Y. Zhang, *European Polymer Journal*, 2009, **45**, 1535-1544.
3. Q. Wang, X. Yao, S. Tang, X. Lu, X. Zhang and S. Zhang, *Green Chemistry*, 2012, **14**, 2559-2566.
4. Q. F. Yue, C. X. Wang, L. N. Zhang, Y. Ni and Y. X. Jin, *Polymer Degradation and Stability*, 2011, **96**, 399-403.
5. C. Jehanno, I. Flores, A. P. Dove, A. J. Müller, F. Ruipérez and H. Sardon, *Green Chemistry*, 2018, **20**, 1205-1212.
6. C. Fan, L. Zhang, C. Zhu, J. Cao, Y. Xu, P. Sun, G. Zeng, W. Jiang and Q. Zhang, *Green Chemistry*, 2022, **24**, 1294-1301.
7. J. Sun, D. Liu, R. P. Young, A. G. Cruz, N. G. Isern, T. Schuerg, J. R. Cort, B. A. Simmons and S. Singh, *ChemSusChem*, 2018, **11**, 781-792.
8. S. Marullo, C. Rizzo, N. T. Dintcheva and F. D'Anna, *ACS Sustainable Chemistry & Engineering*, 2021, **9**, 15157-15165.
9. C. Zhu, L. Yang, C. Chen, G. Zeng and W. Jiang, *Physical Chemistry Chemical Physics*, 2023, **25**, 27936-27941.
10. Z. Wang, Y. Jin, Y. Wang, Z. Tang, S. Wang, G. Xiao and H. Su, *ACS Sustainable Chemistry & Engineering*, 2022, **10**, 7965-7973.
11. S. Brunauer, P. H. Emmett and E. Teller, *Journal of the American Chemical Society*, 1938, **60**, 309-319.

12. J. Hutter, M. Iannuzzi, F. Schiffmann and J. VandeVondele, *WIREs Computational Molecular Science*, 2014, **4**, 15-25.
13. P. Ugliengo, M. Sodupe, F. Musso, I. J. Bush, R. Orlando and R. Dovesi, *Advanced Materials*, 2008, **20**, 4579-4583.
14. J. P. Perdew, A. Ruzsinszky, G. I. Csonka, O. A. Vydrov, G. E. Scuseria, L. A. Constantin, X. Zhou and K. Burke, *Physical Review Letters*, 2008, **100**, 136406.
15. S. Grimme, J. Antony, S. Ehrlich and H. Krieg, *The Journal of Chemical Physics*, 2010, **132**.
16. S. Goedecker, M. Teter and J. Hutter, *Physical Review B*, 1996, **54**, 1703-1710.
17. G. Lippert, J. Hutter and M. Parrinello, *Molecular Physics*, 1997, **92**, 477-488.
18. O. Andreussi, I. Dabo and N. Marzari, *The Journal of Chemical Physics*, 2012, **136**.